

ENLIL+ENKI: Global Context of Heliospheric Simulations

Dusan Odstrcil

June 11, 2004

Contents

1	Introduction	3
2	Solar Wind	3
2.1	Solar Wind Parameters	3
2.2	Numerical Simulations	3
3	Time and Date	4
3.1	Time in Numerical Model	4
3.2	Modified Julian Date	5
3.3	Reference Date	5
4	Coordinate Systems	5
4.1	Description of Coordinate Systems	5
4.1.1	Heliospheric Numerical Model (HNM)	5
4.1.2	Heliocentric Aries Ecliptic (HAE)	5
4.1.3	Heliocentric Earth Ecliptic (HEE)	5
4.1.4	Heliocentric Earth Equatorial (HEEQ)	5
4.1.5	Geocentric Solar Ecliptic (GSE)	6
4.1.6	Heliographic Inertial Coordinate System (HGI)	6
4.1.7	Spacecraft Radial-Tangential-Normal (RTN)	6
4.2	Angles in Heliocentric Coordinate Systems	6
4.2.1	Inclination of the rotation axis to the ecliptic	6
4.2.2	Longitudinal position of the prime meridian	6
4.2.3	Ecliptic longitude	6
4.2.4	Ecliptic longitude of the ascending node	7
4.2.5	Longitude of the Sun's central meridian	7
4.3	Transformation Matrix	7
4.3.1	Single Rotation	7
4.3.2	Eulerian Rotation	7
4.4	Common Transformations in Heliocentric Coordinate Systems	8
4.4.1	HEEQ and HNM	8
4.4.2	HAE and HEEQ	8
4.4.3	HAE and HEE	9
4.4.4	HEEQ and HGI	9
4.4.5	HEE and GSE	9
5	Observational Data	10
5.1	Solar and Coronal Data	10
5.1.1	Solar Rotations	10
5.2	Carrington Rotation Number	10
5.2.1	Solar Pole and Prime Meridian	10
5.2.2	Heliographic Coordinates	10

5.2.3	Heliographic latitude	11
5.2.4	Carrington Longitude	11
5.3	Near-Earth and Interplanetary Data	11
5.3.1	Data Sets for Model Evaluation – NASA/NSSDC/COHOWeb	11
5.3.2	Data Structure	11
6	Numerical Simulations	11
6.1	Background	11
6.2	Heliospheric Simulations	12
7	Using Available Data Sets	13
7.1	Community Data Portal (CDP)	13
7.2	Existing Data Sets	13
8	Using Existing Computational System	13
9	Writing New Computational Procedures	13
10	Installation for Independent Work	13
10.1	System Requirements for ENLIL	13
10.2	System Requirements for ENKI	14
11	Computation of Physical Case - Examples	14
11.1	Analytic Solar Wind	14
11.1.1	Heliospheric Current Sheet	14
11.2	Coupled Corona-Heliosphere	14
11.3	Interacting Flux Ropes	14
11.4	Source Surface Models	14
11.5	Near-Earth Environment	14
12	References	14

1 Introduction

The purpose of this document is to describe a global context of heliospheric simulations relevant to the ENLIL modeling system. There are additional documents describing the organization and structure of data, numerical code, and preparation of input data.

2 Solar Wind

The outermost region of the solar atmosphere, corona, is so hot that the plasma particles can escape gravitational attraction and form a steadily streaming outflow of material called the solar wind. Because of its high temperature, the solar wind is fully ionized plasma consisting primarily of electrons and protons with a minor fraction of helium ions and some other heavier nuclei at several ionization levels. Furthermore, because of the heating and subsequent expansion, the solar wind becomes supersonic above a few solar radii (*Hundhausen, 1972*).

2.1 Solar Wind Parameters

Ambient solar wind can roughly be divided into a slow wind and a fast wind. The slow wind comes from streamer belts, areas of closed magnetic field lines in the Sun. The high speed solar wind is flowing from coronal holes, large areas of open magnetic field lines. Table 2 lists the basic solar wind parameters observed at 1 AU (*Schwenn, 1990*).

The solar rotation causes plasma with different flow speeds eventually to collide and interact with each other. The interaction of slow and fast solar wind at the leading edges of high-speed streams causes compression to high plasma densities and deflections of the flow on both sides of stream interface *Pizzo and Gosling (1998)*. This creates the so-called “corotating interaction regions” (CIR) in the interplanetary space (*Gosling, 1999*). Forward and reverse shock pair is formed usually beyond the 1 AU. Further out separate CIRs may coalesce and produce one larger shock phenomenon called merged interaction region (MIR) (*Gazis, 1991*).

The expanding solar wind drags also the solar magnetic field outward, forming what is called the interplanetary magnetic field (IMF). The solar wind is highly conductive and magnetic field lines are frozen-in to the solar wind flow. Although the solar wind moves out almost radially from the Sun, the rotation of the Sun gives the magnetic field a spiral form. At the Earth orbit the angle between the field lines and the radial is about 45° (*Mariani and Neubauer, 1990*).

Transient disturbances involve coronal mass ejections (CMEs) and interplanetary shocks. Coronal mass ejections (CMEs) represent a huge release of mass into interplanetary space and they have been identified as the primary cause of large, non-recurrent geomagnetic storms (*Gosling, 1990; Hundhausen, 1993*). The propagation speed of interplanetary CMEs can be either extremely low <300 km/s or extremely high >1000 km/s; they may involve a magnetic flux rope structure and they may drive and interplanetary shock.

2.2 Numerical Simulations

We are interested in modeling solar wind phenomena that result in conditions determining geomagnetic storms. Thus, we need to simulate parameters of the magnetic field, flow velocity, mass density, and temperature, for both ambient solar wind and transient disturbances. Figure 1 illustrates the large variations in plasma parameters between the Sun and Earth. Different regions involve different physical phenomena and processes that lead to the development of different models.

On a large scale, it is convenient to distinguish between the “coronal” and “heliospheric” regions with an interface located in the super-critical flow region, usually between 18 and 30 R_S (see Fig. 2). While various plasma heating

Table 1: Typical solar wind parameters observed at 1 AU

Parameter	Slow Stream	Fast Stream
Flow velocity (km/s)	400	700
Proton number density (cm^{-3})	10	3
Proton temperature (kK)	40	200
Magnetic field strength (nT)	4	2

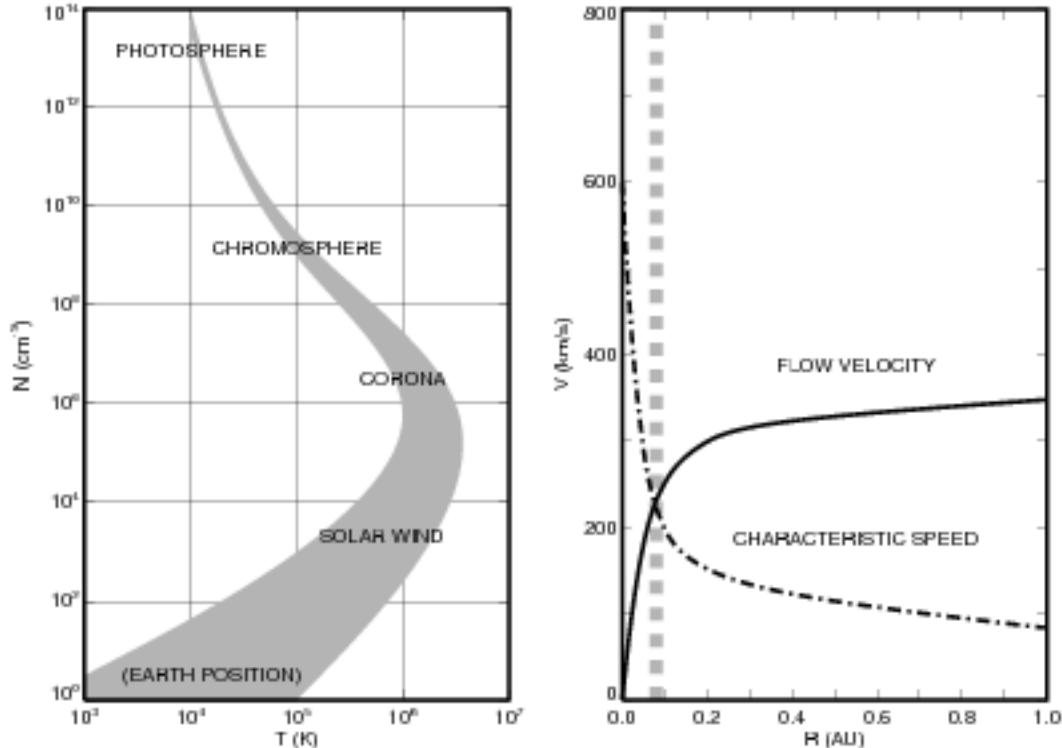


Figure 1: (Left) Diagram of plasma temperature and number density for different regions of space plasma (adapted from D. L. Book, *NRL Plasma Formulary*, NRL Publ. 0084-4040, Washington DC, 1987). (Right) Typical values of the solar wind flow velocity (solid line) and a characteristic speed (the sum of the sound and Alfvén speeds, dash-dotted line) as function of heliocentric distance. Vertical bars show the boundary between sub- and super-critical flow regions.

processes cause acceleration of the solar wind in the corona, it expands mostly adiabatically in the heliosphere. Further, while the background magnetic field plays an important role in the corona, it is passively convected in the heliosphere. Coronal models thus need to simulate more complex physical processes while heliospheric models can use simpler approximations over a much larger spatial domain. Computationally, it is also more efficient to advance the heliospheric portion of the simulation independently of the coronal time step. Note that the location of the model interface in a super-critical region significantly simplifies the numerical treatment of boundary conditions because information is passed only one way: from the coronal model to the heliospheric model.

3 Time and Date

3.1 Time in Numerical Model

Physical time, the quantity `TIME` in the numerical model, is measured in seconds (s). The time interval of a particular numerical simulation is specified by the values of the input parameters `TSTART` and `TSTOP`. The computation starts at `TIME=TSTART` and time is increased by `DTSTEP` during each numerical time step. The computation runs until `TIME ≥ TSTOP`.

Note that `TSTART` can have a negative value. This is useful in computations which require numerical relaxation to achieve an ambient state. In that case, `TSTART` is specified with a negative value, such that at `TIME = 0` an ambient state is surely established in the computational domain and `TIME > 0` is then used for physical simulations.

3.2 Modified Julian Date

Following the astronomical convention, the Julian Date (JD) is defined as the number of days elapsed since January 1, 4713 BCE (i.e., the year -4712) at 12:00 UT plus time expressed as a day fraction. The Modified Julian Date (MJD) is defined as $MJD = JD - 2,400,000.5$ and it is the time measured measured in days from 00:00 UT on 17 November 1858 (Julian Date 2400000.5). We use the MJD since: (1) days begin at midnight rather than noon; (2) for dates in the period from 1859 to about 2130 only five digits need be used to specify the date, rather than seven.

MJD 0 thus corresponds to JD 2,400,000.5, which is twelve hours after noon on JD 2,400,000 = 1858-11-16 (Gregorian or Common Era). Thus MJD 0 designates the midnight of November 16th/17th, 1858, so day 0 in the system of modified Julian day numbers is the day 1858-11-17 CE.

3.3 Reference Date

A reference date is used to relate TIME in the numerical simulation to the calendar date. This reference date is expressed in terms of the Modified Julian Date (MJD) that corresponds to the date when TIME = 0. The value is stored as a global attribute `refdate_mjd` in all input and output NetCDF files. The `refdate_mjd` is thus a parameter that characterizes a particular computational run of a specific event. The actual date is then $MJD = \text{refdate_mjd} + \text{TIME}/86400$. Note that `refdate_mjd` is set to zero for computation of a hypothetical scenario.

4 Coordinate Systems

Various coordinate systems are used to describe locations and vector quantities in numerical simulations and in remote and in-situ observations. The most relevant systems to our needs are listed here together with specification of their orientation angles and common transformations between different systems. Complete description of various coordinate systems has been published by *Russell (1971)*, *Hapgood (1992)*, and *Franz and Harper (2002)*.

4.1 Description of Coordinate Systems

A coordinate system is defined by its origin relative to some other system and by the orientation of its three right-handed axes in space. Note that only two axes needs to be defined; the third axis completes a right-handed Cartesian triad. These systems can be classified according to their origin as heliospheric, geocentric, and spacecraft-centric.

4.1.1 Heliospheric Numerical Model (HNM)

Our numerical model uses a spherical coordinate system where the radius (heliocentric distance, R) is measured from Sun center, meridional angle (co-latitude, θ) is measured down from the north pole (solar rotation axis), and azimuthal angle (longitude, φ) is phased such that the Earth's position is fixed at $\varphi = 180^\circ$. Note that the Earth's position varies in θ due to the 7.25° inclination of the equator to the ecliptic ($R = 1 \text{ AU}$, $\theta = 90^\circ - \text{Bo}$, $\varphi = 180^\circ$).

4.1.2 Heliocentric Aries Ecliptic (HAE)

This coordinate system is defined by the ecliptic plane in which the Earth orbits. The main direction is from the Sun toward the first point of Aries (i.e., toward a point where the Sun is seen from the Earth in the first Spring day). The Earth is located at $R = 1 \text{ AU}$, $\theta = 90^\circ$, $\varphi = \Lambda$.

4.1.3 Heliocentric Earth Ecliptic (HEE)

This coordinate system is defined by the ecliptic plane in which the Earth orbits. The main direction is from the Sun toward the Earth which is located at $R = 1 \text{ AU}$, $\theta = 90^\circ$, $\varphi = 0^\circ$.

4.1.4 Heliocentric Earth Equatorial (HEEQ)

This coordinate system is defined by the solar rotation axis (this defines the solar equatorial plane). The main direction is from the Sun toward the Earth which is located at $R = 1 \text{ AU}$, $\theta = 90^\circ - \text{Bo}$, $\varphi = 0^\circ$.

4.1.5 Geocentric Solar Ecliptic (GSE)

This is a geocentric coordinate system. The X-axis is the Earth-Sun line and the Z-axis points to ecliptic north pole.

Transformation to Geocentric Coordinate Systems. If transformation between other geocentric systems is required, it should be first reduced to a HEE-GSE transformation.

4.1.6 Heliographic Inertial Coordinate System (HGI)

Burlaga (1984) originally defined a system, called heliographic inertial (HGI), which reference to the orientation of the Solar equator in the astronomical epoch J1910.0. This system is used at NASA/COHOweb although another system, heliospheric inertial (HCI) is bases on J2000.0.

The HGI coordinates are Sun-centered and inertially fixed with respect to an X-axis directed along the intersection line of the ecliptic and solar equatorial planes. The solar equator plane is inclined at 7.25° from the ecliptic. This direction was towards ecliptic longitude of 74.367° on 1 January 1900 at 12:00 UT; because of precession of the celestial equator, this longitude increases by $1.4^\circ/\text{century}$. The Z axis is directed perpendicular and northward from the solar equator, and the Y-axis completes the right-handed set.

4.1.7 Spacecraft Radial-Tangential-Normal (RTN)

This coordinate system is centered at a spacecraft or planet and oriented with respect to the line connected the Sun and spacecraft or planet. The R (radial) axis is directed radially away from the Sun through the spacecraft or planet. The T (tangential) axis is the cross product of the Sun's spin vector (North directed) and the R axis, i.e. the T axis is parallel to the solar equatorial plane and is positive in the direction of planetary rotation around the Sun. The N (north) axis completes a right handed system

The RTN coordinates are used at the NASA/NSSDC-COHOWeb archiving system.

4.2 Angles in Heliocentric Coordinate Systems

To carry out coordinate transformations, the various rotation angles are to be known first.

4.2.1 Inclination of the rotation axis to the ecliptic

$$i = 7.25^\circ \quad (1)$$

4.2.2 Longitudinal position of the prime meridian

$$W = (360^\circ/25.38)(\text{JD} - 2398220.0) \quad (2)$$

4.2.3 Ecliptic longitude

This angle corresponds to the azimuthal separation between the Earth and the First Point of Aries. The Sun's ecliptic longitude, Λ , can be calculated using the series of formulae

$$\begin{aligned} T &= (\text{MJD} - 51544.5)/36525 \\ M &= 357.528^\circ + 35999.050^\circ T + 0.04107^\circ h \\ L &= 280.460^\circ + 36000.772^\circ T + 0.04107^\circ h \\ \Lambda &= L + (1.915^\circ - 0.0048^\circ T) \sin(M) + 0.020^\circ \sin(2M) \end{aligned} \quad (3)$$

where T_0 is the time in Julian centuries (36525 days) from 12:00 UT on 1 January 2000 (known as the astronomical epoch J2000.0), M is the Sun's mean anomaly, and L is the mean longitude.

Alternative formulae are

$$\begin{aligned} n &= \text{JD} - 2451545.0 \\ L &= 280.460^\circ + 0.9856474^\circ n \\ g &= 357.528^\circ + 0.9856003^\circ n \\ \Lambda &= L + 1.915^\circ \sin(g) + 0.020^\circ \sin(2g) \end{aligned} \quad (4)$$

where L is the mean longitude, g is the mean anomaly, and n is the number of days from J2000.0 (the astronomical epoch starting on 1 January 2000 at 12:00 UT).

4.2.4 Ecliptic longitude of the ascending node

The ecliptic longitude of the ascending node of the Sun's equator is

$$\Omega = 73.6667^\circ + 0.013958^\circ(\text{MJD} + 3242)/365.25 \quad (5)$$

$$\Omega = 73.6667^\circ + 0.013958^\circ(\text{MJD} + 3243.75)/365.25 \quad (6)$$

4.2.5 Longitude of the Sun's central meridian

The longitude of the Sun's central meridian is

$$\Theta = \text{atan}(\cos(\iota) \tan(\Lambda - \Omega)) \quad (7)$$

4.3 Transformation Matrix

Hapgood (1992) has factorized complex coordinate transformations into series of simple rotations about the principle axis. Only the rotation angle and the name of the rotation axis are required to specify the matrix for a simple rotation. The complex transformation matrix is calculated by multiplication of the simple rotation matrices. This general methodology will be used to provide specific formulae for coordinate transformations in the next Section.

4.3.1 Single Rotation

The notation $S = \langle \alpha, \text{axis} \rangle$ denotes the matrix for a simple rotation, where *angle* is the rotation angle, and *axis* is the rotation axis (X , Y , or Z). The transformation matrix $S = \langle \alpha, X \rangle$ is

$$\begin{array}{lll} S_{00}^X = 1 & S_{10}^X = 0 & S_{20}^X = 0 \\ S_{01}^X = 0 & S_{11}^X = \cos(\alpha) & S_{21}^X = \sin(\alpha) \\ S_{02}^X = 0 & S_{12}^X = -\sin(\alpha) & S_{22}^X = \cos(\alpha) \end{array}$$

and the transformation matrix $S = \langle \alpha, Z \rangle$ is

$$\begin{array}{lll} S_{00}^Z = \cos(\alpha) & S_{10}^Z = \sin(\alpha) & S_{20}^Z = 0 \\ S_{01}^Z = -\sin(\alpha) & S_{11}^Z = \cos(\alpha) & S_{21}^Z = 0 \\ S_{02}^Z = 0 & S_{12}^Z = 0 & S_{22}^Z = 1 \end{array}$$

4.3.2 Eulerian Rotation

Transformations between Cartesian coordinate systems can be realized using the Eulerian transformation matrix. Let systems S^1 and S^2 are defined by the orthogonal right-handed basis vectors X^1, Y^1, Z^1 and X^2, Y^2, Z^2 , respectively. The Eulerian transformation matrix from S^1 to S^2 is defined by three principal rotations such that a vector V^1 given in S^1 has coordinates $V^2 = E * V^1$ in S^2 . All rotation matrices are orthogonal and transformations between all systems defined in this paper can easily be calculated by a series of matrix multiplications.

The HAE to HEEQ transformation is given by the matrix S which comprises: (1) a rotation in the plane of the ecliptic from the First Point of Aries to the ascending node of the solar equator $\langle \Theta, Z \rangle$; (2) then a rotation from the plane of the ecliptic to the plane of the equator $\langle \iota, X \rangle$; and (3) finally a rotation in the plane of the solar equator from the ascending node to the central meridian $\langle \Omega, Z \rangle$.

The resulting transformation matrix, as a matrix multiplication of the previous single rotation matrixes, $S^E = \langle \Theta, Z \rangle \langle \iota, X \rangle \langle \Omega, Z \rangle$. is the so called Eulerian transformation from the ecliptic to the equatorial coordinate systems.

4.4 Common Transformations in Heliocentric Coordinate Systems

The numerical results are stored in the spherical HNM system. Many 3-D visualization tools use data in the Cartesian system. In this case, the conversion HNM \rightarrow HEEQ is necessary. In the HEEQ system, the Earth position is fixed and this is a useful feature. However, some visualizations are better realized in the system in which the Earth and other planets orbits around the Sun. In this case, the conversion HNM \rightarrow HEEQ \rightarrow HAE is necessary. Finally, comparison between numerical results and observations at Earth requires the conversion HNM \rightarrow HEEQ \rightarrow HAE \rightarrow HEE \rightarrow GSE.

The observations at Earth can be stored at the Cartesian GSE system. Sometime these data need to be visualized together with numerical results. In this case, the following conversion is necessary GSE \rightarrow HSE \rightarrow HAE \rightarrow HEEQ. The observations by spacecraft are stored at the RTN system.

4.4.1 HEEQ and HNM

The HNM \rightarrow HEEQ transformation corresponds to a rotation in the plane of the solar equator by -180° and conversion from the spherical geometry to the Cartesian one.

In the Cartesian system, the coordinates are:

$$\begin{aligned} X^{\text{HEEQ}} &= R^{\text{HNM}} \sin(\theta^{\text{HNM}}) \cos(\varphi^{\text{HNM}} + 180^\circ) \\ Y^{\text{HEEQ}} &= R^{\text{HNM}} \sin(\theta^{\text{HNM}}) \sin(\varphi^{\text{HNM}} + 180^\circ) \\ Z^{\text{HEEQ}} &= R^{\text{HNM}} \cos(\theta^{\text{HNM}}) \end{aligned} \quad (8)$$

and the vector components are:

$$\begin{aligned} V_X^{\text{HEEQ}} &= V_R^{\text{HNM}} \sin(\theta^{\text{HNM}}) \cos(\varphi^{\text{HNM}}) + V_\theta^{\text{HNM}} \cos(\theta^{\text{HNM}}) \cos(\varphi^{\text{HNM}}) + V_\varphi^{\text{HNM}} \sin(\varphi^{\text{HNM}}) \\ V_Y^{\text{HEEQ}} &= V_R^{\text{HNM}} \sin(\theta^{\text{HNM}}) \sin(\varphi^{\text{HNM}}) + V_\theta^{\text{HNM}} \cos(\theta^{\text{HNM}}) \sin(\varphi^{\text{HNM}}) + V_\varphi^{\text{HNM}} \cos(\varphi^{\text{HNM}}) \\ V_Z^{\text{HEEQ}} &= V_R^{\text{HNM}} \cos(\theta^{\text{HNM}}) - V_\theta^{\text{HNM}} \sin(\theta^{\text{HNM}}) \end{aligned} \quad (9)$$

4.4.2 HAE and HEEQ

The HAE \rightarrow HEEQ transformation comprises of three rotations that have been composed into the transformation matrix S as specified in Section 4.3. Vector components are:

$$\begin{aligned} V_X^{\text{HAE}} &= V_X^{\text{HEEQ}} (\cos(\Theta) \cos(\Omega) - \sin(\Theta) \cos(\iota) \sin(\Omega)) + V_Y^{\text{HEEQ}} (\sin(\Theta) \cos(\Omega) + \cos(\Theta) \cos(\iota) \sin(\Omega)) \\ &\quad + V_Z^{\text{HEEQ}} \sin(\iota) \sin(\Omega) \\ V_Y^{\text{HAE}} &= V_X^{\text{HEEQ}} (-\cos(\Theta) \sin(\Omega) - \sin(\Theta) \cos(\iota) \cos(\Omega)) + V_Y^{\text{HEEQ}} (-\sin(\Theta) \sin(\Omega) + \cos(\Theta) \cos(\iota) \cos(\Omega)) \\ &\quad + V_Z^{\text{HEEQ}} \sin(\iota) \cos(\Omega) \\ V_Z^{\text{HAE}} &= V_X^{\text{HEEQ}} \sin(\Theta) \sin(\iota) - V_Y^{\text{HEEQ}} \cos(\Theta) \sin(\iota) + V_Z^{\text{HEEQ}} \cos(\iota) \end{aligned} \quad (10)$$

The HEEQ \rightarrow HAE transformation comprises of three rotations that have been composed into the transformation matrix S as specified in Section 4.3. Vector components are:

$$\begin{aligned} V_X^{\text{HEEQ}} &= V_X^{\text{HAE}} (\cos(\Theta) \cos(\Omega) - \sin(\Theta) \cos(\iota) \sin(\Omega)) + V_Y^{\text{HAE}} (-\cos(\Theta) \sin(\Omega) - \sin(\Theta) \cos(\iota) \cos(\Omega)) \\ &\quad + V_Z^{\text{HAE}} \sin(\Theta) \sin(\iota) \\ V_Y^{\text{HEEQ}} &= V_X^{\text{HAE}} (\sin(\Theta) \cos(\Omega) + \cos(\Theta) \cos(\iota) \sin(\Omega)) + V_Y^{\text{HAE}} (-\sin(\Theta) \sin(\Omega) + \cos(\Theta) \cos(\iota) \cos(\Omega)) \\ &\quad - V_Z^{\text{HAE}} \cos(\Theta) \sin(\iota) \\ V_Z^{\text{HEEQ}} &= V_X^{\text{HAE}} \sin(\iota) \sin(\Omega) + V_Y^{\text{HAE}} \sin(\iota) \cos(\Omega) + V_Z^{\text{HAE}} \cos(\iota) \end{aligned} \quad (11)$$

4.4.3 HAE and HEE

The HAE \rightarrow HEE transformation corresponds to a rotation in the plane of the ecliptic from the Sun-Earth direction to the First Point of Aries. In the spherical geometry, the azimuthal coordinates are shifted by $-A$ and the vector components are unchanged. In the Cartesian geometry, the coordinates and vector components are:

$$\begin{aligned} V_X^{\text{HAE}} &= V_X^{\text{HEE}} \cos(A + 180^\circ) - V_Y^{\text{HEE}} \sin(A + 180^\circ) \\ V_Y^{\text{HAE}} &= V_X^{\text{HEE}} \sin(A + 180^\circ) + V_Y^{\text{HEE}} \cos(A + 180^\circ) \\ V_Z^{\text{HAE}} &= V_Z^{\text{HEE}} \end{aligned} \quad (12)$$

The HEE \rightarrow HAE transformation corresponds to a rotation in the plane of the ecliptic from the First Point of Aries to the Sun-Earth direction. In the spherical geometry, the azimuthal coordinates are shifted by A and the vector components are unchanged. In the Cartesian geometry, the coordinates and vector components are:

$$\begin{aligned} V_X^{\text{HEE}} &= V_X^{\text{HAE}} \cos(A + 180^\circ) + V_Y^{\text{HAE}} \sin(A + 180^\circ) \\ V_Y^{\text{HEE}} &= -V_X^{\text{HAE}} \sin(A + 180^\circ) + V_Y^{\text{HAE}} \cos(A + 180^\circ) \\ V_Z^{\text{HEE}} &= V_Z^{\text{HAE}} \end{aligned} \quad (13)$$

4.4.4 HEEQ and HGI

The HEEQ \rightarrow HGI transformation corresponds to a rotation in the plane of the solar equator from the Sun-Earth direction to the ascending node of the ecliptic.

$$\begin{aligned} V_X^{\text{HGI}} &= V_X^{\text{HEEQ}} \cos(A - \Omega) + V_Y^{\text{HEEQ}} \sin(A - \Omega) \\ V_Y^{\text{HGI}} &= -V_X^{\text{HEEQ}} \sin(A - \Omega) + V_Y^{\text{HEEQ}} \cos(A - \Omega) \\ V_Z^{\text{HGI}} &= V_Z^{\text{HEEQ}} \end{aligned} \quad (14)$$

The HGI \rightarrow HEEQ transformation corresponds to a rotation in the plane of the solar equator from the ascending node of the ecliptic to the Sun-Earth direction.

$$\begin{aligned} V_X^{\text{HEEQ}} &= V_X^{\text{HGI}} \cos(A - \Omega) + V_Y^{\text{HGI}} \sin(A - \Omega) \\ V_Y^{\text{HEEQ}} &= -V_X^{\text{HGI}} \sin(A - \Omega) + V_Y^{\text{HGI}} \cos(A - \Omega) \\ V_Z^{\text{HEEQ}} &= V_Z^{\text{HGI}} \end{aligned} \quad (15)$$

4.4.5 HEE and GSE

Conversion between the heliocentric and geocentric systems is best defined between HEE and GSE systems, as these are very simply related. The transformation HEE \rightarrow GSE is:

$$\begin{aligned} V_X^{\text{HEE}} &= -V_X^{\text{GSE}} \\ V_Y^{\text{HEE}} &= -V_Y^{\text{GSE}} \\ V_Z^{\text{HEE}} &= V_Z^{\text{GSE}} \end{aligned} \quad (16)$$

and the transformation GSE \rightarrow HEE is:

$$\begin{aligned} V_X^{\text{GSE}} &= -V_X^{\text{HEE}} \\ V_Y^{\text{GSE}} &= -V_Y^{\text{HEE}} \\ V_Z^{\text{GSE}} &= V_Z^{\text{HEE}} \end{aligned} \quad (17)$$

Transformations for other geocentric systems is beyond the scope of this document (see *Russell, 1984; Hapgood, 1998* for details).

5 Observational Data

5.1 Solar and Coronal Data

The main coordinate systems are:

- heliographic – refers to coordinates on the solar surface referenced to the solar rotational axis
- sidereal – refers to a coordinate system fixed with respect to the distant stars.
- synodic – refers to a coordinate system fixed on the Earth.

5.1.1 Solar Rotations

For the solar rotation period the adopted values are

$$T_{\text{sid}} = 25.38 \text{ days} \quad (18)$$

$$T_{\text{syn}} = 27.2753 \text{ days} \quad (19)$$

where the sidereal period T_{sid} is relative to the celestial sphere and the synodic relative to the orbiting Earth.

Rotations of the Sun are counted in Carrington rotations CR that starts when the heliographic prime meridian crosses the sub-terrestrial point of the solar disc. The angular offset θ between this point and the ascending node can be calculated from

$$\theta = \arctan(\cos(\epsilon) \tan(\lambda - \Omega)) \quad (20)$$

such that the quadrant of θ is opposite that of $\lambda - \Omega$. The first Carrington rotation started on 9 November 1853 (JD 2398167.329). Later start points can be calculated using the synodic period $T_{\text{syn}} = 27.2753$ days.

The heliographic longitude system corresponds to the average rotation of equatorial regions.

5.2 Carrington Rotation Number

The Carrington rotation number corresponding to a particular Julian date may be derived from

$$CR = 1750 + \text{int} \left(\frac{\text{MJD} - 45871.41}{27.2753} \right) \quad (21)$$

where int denotes the integer part. Rotation number 1750 began on 1984 June 20.41.

5.2.1 Solar Pole and Prime Meridian

Heliographic coordinate systems use the position of the solar rotation axis which is defined by its declination δ and the right ascension α with respect to the celestial pole. Values for J2000.0 are

$$\delta = 63.87^\circ, \alpha = 286.13^\circ$$

The traditional definition refers to the ecliptic plane of date with the values for the inclination I of the solar equator and longitude of the ascending node Ω

$$I = 7.25^\circ, \Omega = 75.76^\circ + 1.397^\circ T_0$$

5.2.2 Heliographic Coordinates

B_0 – Heliographic latitude of the central point of the solar disk; also called the B-angle. The range of B_0 is $\pm 7.25^\circ$, correcting for the tilt of the ecliptic with respect to the solar equatorial plane.

L_0 – Heliographic longitude of the central point of the solar disk. The longitude value is determined with reference to a system of fixed longitudes rotating on the Sun at a rate of $13.2^\circ/\text{day}$ (the mean rate of rotation observed from central meridian transits of sunspots).

The standard meridian on the Sun is defined to be the meridian that passed through the ascending node of the Sun's equator on 1 January 1854 at 1200 UTC and is calculated for the present day by assuming a uniform sidereal period of rotation of 25.38 days.

Longitude of the ascending node: $\Omega = 73^\circ 40' + 50.25'' (\text{JD} - 2396756.75)/365.25$

heliographic latitude:

$$\text{Bo} = \frac{\pi}{2} - \arctan(\sin(\text{Bo})/\cos(\text{Bo}))$$

where $\sin(\text{Bo}) = \sin(\lambda - \Omega)\pi/180^\circ \sin(I\pi/180^\circ)$ and $\cos(\text{Bo}) = (1 - (\sin(\text{Bo}))^2)^{1/2}$

5.2.3 Heliographic latitude

The heliographic latitude (i.e., the central point of the solar disk as seen from the Earth). This angle corresponds to the meridional separation between the solar equatorial plane and the Earth's position.

$$\text{Bo} = 90^\circ - \arctan\left(\frac{\sin(\text{Bo})}{\cos(\text{Bo})}\right) \quad (22)$$

where $\sin(\text{Bo}) = \sin(\lambda - \Omega) \sin(i)$, $\cos(\text{Bo}) = (1 - (\sin(\text{Bo}))^2)^{1/2}$, and longitude of the ascending node $\Omega = 73^\circ 40' + 50.25'' (\text{MJD} + 3243.75)/365.25 (= 73^\circ 40' + 50.25'' (\text{JD} - 2396756.75)/365.25)$.

5.2.4 Carrington Longitude

The heliographic longitude system corresponds to the average rotation of equatorial regions.

A system of fixed solar longitudes rotating at a uniform synodic period of 27.2753 days (a sidereal period of 25.38 days). Carrington selected the meridian that passed through the ascending node of the Sun's equator at 12:00 UTC on 1 January 1854 as the original prime meridian.

5.3 Near-Earth and Interplanetary Data

5.3.1 Data Sets for Model Evaluation – NASA/NSSDC/COHOWeb

These data sets are a compilation of observations of heliospheric events, which are a start to be used in the evaluation of numerical heliospheric models. The main purpose is to enable prompt comparison between numerical results and observed data. First steps, mostly for numerical modelers, Data gaps. Real model validation and/or analysis of observations requires using detail original data bases and specialized data processing and visualization procedures.

The data sets are stored as NetCDF files at the same location as numerical results to facilitate direct comparison using the same data processing and visualization tools. There are the following data sets:

- Observations of solar wind parameters at Earth from 1990 to present (extracted from the NASA/COHOWeb data base <http://nssdc.gsfc.nasa.gov/cohoweb/cw.html>) These observations are hourly averaged and contains the following quantities: particle number density, mean temperature, components flow velocity, total magnetic field and its components, as well as location of Earth and time.

5.3.2 Data Structure

S/C Distance (Heliocentric) S/C Latitude (HGI) S/C Longitude (HGI) BR in RTN BT in RTN BN in RTN
B Magnitude Plasma Velocity Proton Density Proton Temperature

6 Numerical Simulations

6.1 Background

Traditionally, individuals and groups have developed numerical codes and then either they applied them to physical problems themselves, or they provided them to other groups for installation and application. The first approach is very efficient; however, only limited involvement of external individuals or group is possible via run-on-request due

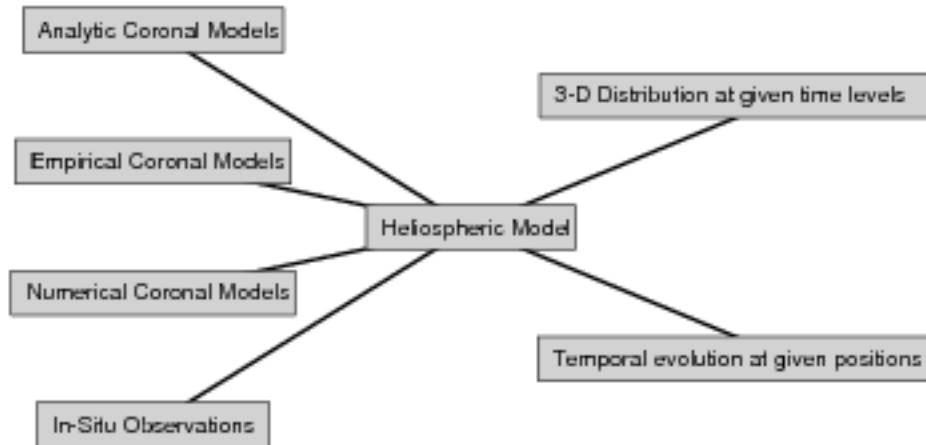


Figure 2: Basic schema.

to time constraints of the code originator(s). The second approach significantly expands the capability of applying the code(s) to a variety of physical problems; however, it is more demanding on the user side, especially with more complex codes and parallel computer systems, as well as the code originator(s).

Recent advances in the Internet and Grid technologies makes it possible maintain the codes centrally and to utilize them remotely. This simplifies maintenance of research codes that are under continual development (to incorporate more physics, better numerics, and efficient usage of system resources). Moreover, this new approach is attractive to a much broader community than the traditional approach. For example, an individual might be interested in: (1) utilizing existing results from simulations of specific events to compare with observations, (2) re-running existing simulations but with different parameters, (3) experimenting with various initialization procedures to drive simulations, or (4) visualizing events for educational purposes. Such activities do not require detailed understanding of the mathematical model, numerical methods, code structure, programming languages, computational systems, etc.

6.2 Heliospheric Simulations

There are various ways to use heliospheric simulations to meet particular needs of individual researchers, students, and educators:

- Installation for independent work. Implement the code on the local computational system and use it for new applications (see Section 10).
- Using available data sets. Visualize, analyze, and utilize a large collection of data sets obtained during simulation of representative periods and events (see Section 7).
- Using available modeling system. Prepare input data using existing initialization procedures and data sets and configure the existing numerical model (see Section ??).
- Writing new initialization procedures. Develop new initialization procedures to produce input data for the code, incorporate them into the ENKI portal, and run the existing numerical model (see Section ??).
- Writing new computational procedures. Develop new computational procedures, incorporate them into the ENLIL modeling system as well as the ENKI portal, and use the existing initialization system to run the modified code (see Section 9).

The first two items in the list provide a simple and fast way to access heliospheric data sets that might be useful to educators and for analysis of observational data. Subsequent list items demand increasing familiarity with the ENLIL modeling system; however, the user acquires more flexibility in studying new physical problems.

7 Using Available Data Sets

7.1 Community Data Portal (CDP)

Results from selected numerical simulations are archived as data sets at the NCAR Supercomputer Center in Boulder, CO. These data sets are available via the Community Data Portal (CDP) that provides an interactive access to browsing, pre-viewing, and downloading of data sets. The CDP can be accessed at <http://dataportal.ucar.edu:8443/cdp/index.html> where the user is asked for registration.

7.2 Existing Data Sets

Data sets accessible via CDP involve:

- interaction between a plasma cloud and the tilted heliospheric streamer belt;
- ambient solar wind driven by the WSA empirical model;
- ambient solar wind driven by the SAIC semi-empirical model;
- interplanetary flux rope driven by the SAIC coronal model;
- selected interplanetary CME events driven by the cone model.

Prospective users should check the CDP for the latest content, as the archive is continually updated.

8 Using Existing Computational System

9 Writing New Computational Procedures

CVS (Concurrent Versions System) is the open-source network-transparent version control system (<http://www.cvshome.org>).

10 Installation for Independent Work

Different systems will require modifications to configuration files. Further, lack of MPI, NetCDF, Perl, and IDL libraries and different computer architecture may require complete rewriting of i/o procedures and number-crunching subprograms.

10.1 System Requirements for ENLIL

You should have the following:

- Fortran 95 (or 90) compiler;
- CPP pre-processor;
- MPI (Message-Passing Interface) library;
- NetCDF (Network Common Data Format) library;
- PARAMESH library;
- A copy of the ENLIL source code distribution.

10.2 System Requirements for ENKI

You should have the following:

- IDL (Interactive Data Language from Research Systems Inc.)
- Perl;
- Apache web server (enabling cgi-bin commands);
- A copy of the ENKI source code distribution.

11 Computation of Physical Case - Examples

11.1 Analytic Solar Wind

11.1.1 Heliospheric Current Sheet

$$z2 = \theta * \tan(A_{sheet}) + B_{sheet} * \sin(\theta) \quad (23)$$

if $\theta < z2 - 0.5 \text{ wsheet}$:

$b1lv = -b1c$
 $b2lv = -b2c$

if $z2 - 0.5 \text{ wsheet} < \theta < z2 + 0.5 \text{ wsheet}$:

$b1lv = 0$
 $b2lv = 0$
 $Pmag = \text{const}$

11.2 Coupled Corona-Heliosphere

11.3 Interacting Flux Ropes

11.4 Source Surface Models

11.5 Near-Earth Environment

12 References

- Arge C. N., and V. J. Pizzo, Improvement in the prediction of solar wind conditions using near-real time solar magnetic field updates, *J. Geophys. Res.*, *105*, 10,465-10,480, 2000.
- Franz, M., and D. Harper, Heliospheric coordinate systems, *Planet. Space Sci.*, *50* 217, 2002.
- Franz, M., and D. Harper, Corrections for Heliospheric coordinate systems, *Planet. Space Sci.*, ?? ???, 200?.
- Hapgood, M., Space physics coordinate transformations: A user guide, *Planet. Space Sci.*, *40*, 711-717, 1992.
- Hapgood, M., Corrigendum, Space physics coordinate transformations: A user guide, *Planet. Space Sci.*, *45*, 1047, 1992.
- Hundhausen, A. J., Coronal Expansion and Solar Wind, Springer Verlag, New York, 1972.
- Hundhausen, A. J., Size and locations of coronal mass ejections: SMM observations from 1980 and 1984-1989, *J. Geophys. Res.*, *98*, 13,177-13,200, 1993.
- Mariani, F., and F. M. Neubauer, The interplanetary magnetic field, in: *Physics of the Inner Heliosphere* eds. R. Schwenn and E. Marsch, pp. 183-206, Springer Verlag, New York, 1990.

Russell, C. T., Geophysical coordinate transformations, *Cosmic Electrodyn*, 2 184, 1971.

Schwenn, R., Large-scale structure of the interplanetary medium, in: *Physics of the Inner Heliosphere* eds. R. Schwenn and E. Marsch, pp. 99-181, Springer Verlag, New York, 1990.